Cluster motion on surfaces: A stochastic model*

Uzi Landman[†] and Michael F. Shlesinger[†]

*Department of Physics and Astronomy, Institute of Fundamental Studies, University of Rochester,
Rochester, New York 14627*
(Received 14 April 1977)

A stochastic model of the diffusion of clusters on crystalline surfaces is presented. The cluster configurations are mapped onto a periodic lattice with internal states. The formulation is capable of treating complex kinetics, cluster structures, and surface topologies. A detailed analysis of dimers with two and three allowable states in one and two dimensions is given. These correspond to recent observations of the diffusion of atomic clusters on surfaces by field-ion microscopy techniques. Expressions for the transition rates between spatial configurations involved in the motion of the clusters are derived in terms of experimental observables. It is demonstrated that for a complete determination of the parameters characterizing the various cluster configurations (i.e., activation energies and frequency factors) full use of the field-ion microscope data (moments of the cluster centroid displacement and equilibrium-state occupation probabilities) is required. The effect of a bias field is included in our analysis, and shown to be essential in certain cases for a complete determination of the transition rates. The effect of periodically placed defects on the diffusion on surfaces is investigated.

I. INTRODUCTION

In recent years investigations of surface phenomena have constituted a major thrust of scientific endeavor. While being a topic of interest and relevance for many years, the modern approaches to the subject are characterized by an emphasis on a microscopic level of description.[1] Such studies which aim at the interpretation and construction of theoretical models of fundamental interaction processes occurring at material surfaces are greatly enhanced by advances in experimental techniques which allow the observation of surface structure and interaction phenomena on a microscopic scale. In investigations of the interactions of atomic species with solid surfaces and between atomic species mediated by a surface, it is recognized that in order to achieve a proper description of the system the individual and correlated effects of several factors have to be studied. These factors include surface geometrical structure, electronic and vibronic spectra, dynamics, kinetics, and thermodynamical considerations.[2,3] As a starting point for a discussion of chemical reactions on solid surfaces, it is convenient to postulate a schematic series of "elementary" reaction steps: adsorption, migration, and desorption. While the term "heterogeneous catalytic reaction"[4] is customarily reserved for the interaction between atomic species in the presence of a surface when the atomic reactants originate in the gaseous (or liquid) phase, it could be generalized to describe various surface processes such as annealing and sintering[5] thin-film growth,[6] etc., in which one or more of the "elementary" reaction steps may be missing. Reactions may be classified according to

rate-limiting steps in the reaction mechanism. The identification of the rate-limiting steps and their dependence on the characteristics of the system and reaction under study are of major importance in the construction of kinetic schemes, and for establishing classification trends according to the type of reactions and reactants considered. The complexity and versatility of surface systems complicates the definition of the "elementary steps" to such a degree that the study of each of them separately forms a subfield of considerable complexity both experimentally and theoretically. The ultimate goal of surface studies is to relate and correlate the various phenomena in a coherent scheme. A possible approach for the construction of a general theory of reactions on surfaces is within a statistical thermodynamical stochastic framework.[7,8] This approach, which proved to be most successful in investigations of the kinetics of chemical reactions, is particularly suitable for the study of heterogeneous catalytic reactions which involve the interaction of atomic and molecular species with condensed-matter systems. In attempting to advance beyond a thermodynamical macroscopic description, it would be necessary to express thermodynamical quantities such as the free energy in terms of microscopic models of the interaction processes. In order to be able to test and assess theoretical models it is essential that methods for the analysis of experimental data be developed. The degree of detail required of the analysis techniques is often dictated by the nature of the experiment. In addition, such studies may suggest either new experiments or modifications of existing techniques.

In this paper we employ stochastic techniques

for the study of the migration of clusters on crys-
talline surfaces. Our study was motivated by
recent observations[9] of the correlated motion of
atoms on metal surfaces using field-ion-micro-
scopy[10] (FIM) techniques. Thus, the main objec-
tive of the present paper is to study the above
phenomenon and suggest methods for analyzing
the wealth of FIM experimental data, and to sug-
gest new experiments to enable the extraction of
parameters which characterize the motion.[11] Add-
itionally, the formalism which we developed is a
rather general one such as to provide a frame-
work for the study of reactions on surfaces along
the lines discussed above.

The challenging goal of observing individual
atoms on surfaces was first achieved upon the in-
troduction of the field-ion microscope by Müller
over two decades ago.[12] In recent years other
methods for the imaging of individual atoms, such
as transmission-electron microscopy operated in
either bright- or dark-field modes and high-reso-
lution electron-microscopy techniques, have been
developed.[13] While these techniques may extend
the range of materials to which the FIM method
can be applied, the latter one remains the major
source of quantitative data of atomic resolution.
In particular, data about the migration of individual
species on surfaces is currently available only
from FIM measurements. Nevertheless, the re-
sults which we present in the following are not
limited to the analysis of FIM data.

FIM observations of correlated motion of clus-
ters of atoms on metal-surface planes is one of
the most significant results in recent work on sur-
face diffusion. The observation of this phenomen-
on indicates the importance of interactions be-
tween adatoms on metal surfaces in controlling
the mechanisms for their migration. Clearly, to
describe the correlated motion and enable the ex-
traction of physical quantities from the data a new
theoretical formulation is needed.[9(d)] Apart from
explaining the experimental data and suggesting
new experiments, the analysis may be of relevance
in comparing and evaluating theoretical models of
adatom-adatom interactions (direct and substrate
mediated) on metal surfaces[14-16] by virtue of pro-
viding quantitative measures of parameters (like
activation energies of migration and frequency
factors) which enter the description of related
phenomena. Since detailed descriptions of FIM
techniques and statements of the "state of the
art" are available in the literature (see Refs. 9
and 10), we restrict ourselves to a very brief des-
cription of the available data of cluster diffusion
on metal surfaces. (The following list is by no
means exhaustive; for additional examples, the
reader should consult the bibliography cited in

Ref. 9.) First, we note that cluster diffusion on
metal surfaces was observed for systems exhibit-
ing variable cluster sizes and dimensionality of the
motion. As examples, we mention one-dimension-
al motion of tungsten[9(c),17-21] and rhenium[22] dimers
on W(211) and tungsten triplets[18(b)] on the same
substrate, two-dimensional motion of tungsten[23]
dimers on the (110) face of tungsten, and the mo-
tion of higher-order clusters of ihridium[25] and
platinum[23-25] on W(110).

Most schematically, FIM studies of the migra-
tion of adatoms involve[9,22] the evaporation of a
few atoms onto the field emitter tip, followed by
measurements of their motion after successive
periods of heating. (The typical range of tempera-
ture is of the order ~100 °K.) During a heating
stage (typically 20–90 s, depending on tempera-
ture), the high electric field used for imaging is
absent to avoid the effect of the field. The imag-
ing stage is done at a cryogenic temperature of
~20 °K to ensure a freezing of the motion. To ob-
tain well-characterized contaminant-free condi-
tions the experiments are performed in an ultra-
high-vacuum environment. From the chronologi-
cal series of micrographs a mapping of positions
is performed from which an assignment and tabu-
lation of adatom displacements is made. In order
to be able to construct a statistical sample, ap-
proximately ~100 observations are made at each
temperature. From the resulting histograms the
variance of the displacement and the mean posi-
tions (available if experiments are done under
the influence of a bias field) can be determined as
a function of temperature. In addition, analysis of
the micrographs provides data about the equilib-
rium occupation probabilities of the various states
which the migrating species encounters during its
motion. As will be discussed in the following sec-
tions, to enable a complete characterization of the
diffusion process, *full use must be made of the
FIM data,* and in certain cases experiments under
the influence of a bias field are *necessary.*[11]

As indicated above, it is observed that the mi-
gration of clusters on crystalline metal surfaces
proceeds via transitions between possible cluster
configurations. The nature of the motion and the
allowed spatial configurations depend upon the
substrate morphology and composition and the
composition and size of the migrating cluster
(these factors are related, of course, to the ener-
getics of the system, i.e., adsorbate-substrate
and interadsorbate interactions). A cluster will be
characterized by the number of states (configura-
tions) which participate in its motion, by its size,
and by the dimensionality of the motion. In Figs.
1(a) and 2(a) cluster configurations (in coordinate
space) are shown for dimer migration in one and

ID DIMER

(a)

ID 3 STATE DIMER

(b)

ID 2 STATE DIMER
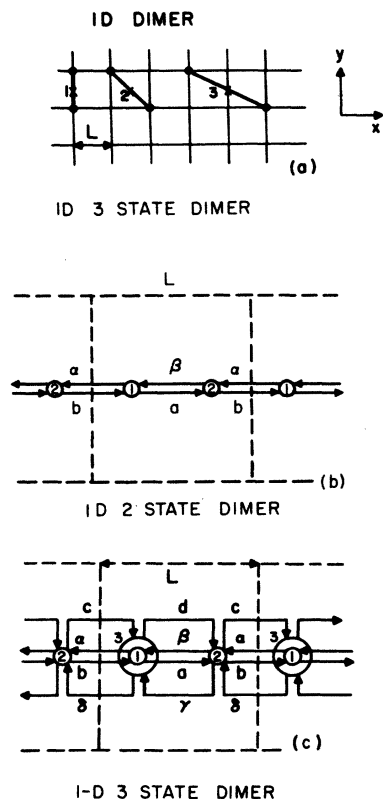

(c)

I-D 3 STATE DIMER

FIG. 1. One-dimensional dimer migration. (a) Three possible spatial configurations of a dimer (filled circles connected by heavy line) moving along the x direction (the allowed equivalent mirror-image configurations are not included): if only states 1 and 2 are allowed, a 2-state dimer; if all states are allowed, a 3-state dimer. The location of the dimer centroid is marked ✕. (b) Random-walk lattice describing the motion of the centroid of a 2-state in (a). The unit cell is denoted by dashed lines and the states by numbered circles. Lettered arrows indicate transitions to and from states. Note that transition rates connecting states can be different for transitions to the left or right (i.e., $a \neq \alpha$, $b \neq \beta$). (c) Random-walk lattice for the 3-state dimer shown in (a). Note that the centroid location is the same for states 1 and 3; however, they are distinguished by different transition rates.

two dimensions, respectively (on a rectangular lattice). In Fig. 1(a), if all three states are allowed, the dimer is called a one-dimensional (1-D) 3-state dimer; if state 3 is prohibited, the diagram describes a 1-D 2-state dimer. The system shown in Fig. 2(a) is characterized as a 2-D 3-state dimer. The motion of a cluster is best described in terms of the location of the centroid of the cluster [denoted by ✕ in Figs. 1(a) and 2(a)], which can be *mapped* onto a periodic lattice on which it performs a random walk. Such mappings are shown in Figs. 1(b) and 1(c) for the 1-D 2-state and 1-D 3-state dimers, respectively, and
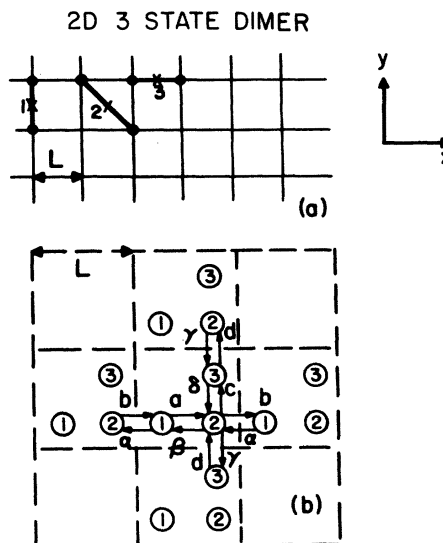
2D 3 STATE DIMER

(a)

(b)

FIG. 2. Two-dimensional dimer migration: (a) spatial configurations; (b) random-walk lattice.

in Fig. 2(b) for the 2-D 3-state dimer. It is observed that the unit cell of the random-walk lattice (denoted by the dashed lines) contains, generally, several "sites" or internal states (denoted by numbered circles). The transition rates between the states are designated by lettered arrows. In addition, by allowing for different transition rates in and out of states (i.e., $a \neq \alpha$, $b \neq \beta$, etc.) a directional preference (bias) to the motion can be introduced. In the case of the 1-D 3-state dimer [Fig. 1(c)] it should be noted that the spatial locations of the centroid of states 1 and 3 coincide; however, they are distinguished by different transition rates. Such situations, which occur often in the analysis of higher-order clusters, could not be treated by previous methods.[26] As we have discussed elsewhere,[11] and as shown in the following sections, the inclusion of the third state modifies the expressions for the motion of the cluster. Since the forces holding atomic clusters together involve long-range contributions, it is expected that extended configuration such as the one shown in Fig. 1(a) (state 3) can occur. Consequently, FIM data should be carefully examined for such occurrences and analyzed accordingly.

In this paper we describe a formalism, based on stochastic-processes techniques, which we apply to the problem of cluster motion on surfaces. Furthermore, we obtain explicit expressions for the transition rates between the individual cluster states in terms of observable quantities. In Sec. II A we outline the mathematical formulation of the "continuous-time random walk with internal states" method.[27] Section II B contains a

concise description of the procedure which we use. Case studies of cluster diffusion on crystalline surfaces are discussed in Sec. III, in which some details of the calculations are exhibited. In Sec. IV we present formulas for the transition rates in terms of observable quantities, and discuss aspects of the analysis of experimental data. Finally, in Sec. V motion on defective lattices is discussed. These systems are of particular interest in studies of poisoning or deactivation of catalytic-diffusion-controlled processes, and in investigations of the role of active sites in surface-diffusion-controlled reactions.

II. CONTINUOUS-TIME RANDOM WALK WITH INTERNAL STATES AND THE DIFFUSION LIMIT

A. Mathematical formulation

To describe the random motion of a particle on periodic lattices in which each cell contains a number of internal states (see Figs. 1 and 2) a generalization of the continuous-time random-walk (CTRW) formalism[28-31] is required. Since a detailed description of such a generalized formulation was discussed by us recently,[27] we limit ourselves in this section to a presentation of the underlying principles of the method and provide a concise procedure for its application.

Consider a d-dimensional periodic space lattice of identical cells, each being identified by a vector

$$\vec{S} = (s_1, s_2, \ldots, s_d), \quad \text{with } s_\alpha = 1, 2, \ldots, N_\alpha \quad (2.1)$$

where in most applications $N_\alpha \to \infty$ for all α. Within a cell, internal states labeled by an index $j = 1, \ldots, m$ are available to the walker.

The basic quantity of concern is the probability

$$P_{j, j_0}(\vec{S}, \vec{S}_0; t) \quad (2.2)$$

that a walker created at time $t = 0$ in cell $\vec{S}_0$ in state j_0 will be in cell $\vec{S}$ in state j at time t. [In the following the couple $(\vec{S}, j)$ represents state j in cell $\vec{S}$.] In the study of P it is convenient to define also the probability

$$Q^{(n)}_{j, j_0}(\vec{S}, \vec{S}_0; t) \quad (2.3)$$

that a walker created at $t = 0$ in $(\vec{S}_0, j_0)$ makes its nth transition achieving $(\vec{S}, j)$ *exactly* at time t. The probability $Q_{j, j_0}(\vec{S}, \vec{S}_0; t)$ that the walker created at $t = 0$ in $(\vec{S}_0, j_0)$ will reach $(\vec{S}, j)$ *exactly* at time t via *any* available path is given as

$$Q_{j j_0}(\vec{S}, \vec{S}_0; t) = \sum_{n=0}^{\infty} Q^{(n)}_{j j_0}(\vec{S}, \vec{S}_0; t). \quad (2.4)$$

Both P and Q can be described in terms of a transition probability $\psi_{j j'}(\vec{S}, \vec{S}'; \tau)$ which characterizes each step. Let us assume for ψ the form

$$\psi_{j j'}(\vec{S}, \vec{S}'; \tau) d\tau \equiv F_{j j'}(\vec{S}, \vec{S}'; \tau) \psi_{j'}(\tau) d\tau, \quad (2.5)$$

where $\psi_j(\tau) d\tau$ is the probability that if the walker reached state j at time $t = 0$, then it will leave it (independent of the cell $\vec{S}$) in the time interval $(\tau, \tau + d\tau)$; i.e., $\psi_j(\tau)$ is a waiting-time density function. For the transition occurring at time τ the F function in the above equation is the probability of $(\vec{S}', j') \to (\vec{S}, j)$ in *one step* at time τ. The associated normalization conditions are

$$\sum_{j, \vec{S}} F_{j j'}(\vec{S}, \vec{S}'; \tau) = 1 \text{ and } \int_0^\infty \psi_j(\tau) d\tau = 1. \quad (2.6)$$

We note that the doubly subscripted quantities can be arranged into $m \times m$ matrices, and the ψ_j's form a diagonal matrix of the same order.

The n-step walk carrying the walker from $(\vec{S}', j')$ to $(\vec{S}, j)$ with the precise arrival time τ satisfies the matrix recursion relation

$$\underline{Q}^{(n+1)}(\vec{S}; \tau) = \sum_{\vec{S}'} \int_0^\tau \underline{Q}^{(n)}(\vec{S} - \vec{S}'; \tau - \tau') \underline{\psi}(\vec{S}'; \tau') d\tau', \quad (2.7)$$

where translational invariance of the system has been assumed. We define now the discrete Fourier transform of a function $f(\vec{S})$ as

$$f^*(\vec{k}) \equiv \frac{1}{N_1 \cdots N_d} \sum_{s_1 = 1}^{N_1} \cdots \sum_{s_d = 1}^{N_d} f(\vec{S}) \exp[i(\vec{k} \cdot \vec{S})], \quad (2.8)$$

where $\vec{k} \equiv (2\pi r_1/N_1, \ldots, 2\pi r_d/N_d)$ and $\vec{S}$ is given in Eq. (2.1). Also the Laplace transform of a function $g(t)$ over the continuous variable t is defined to be

$$\tilde{g}(u) \equiv \int_0^\infty e^{-tu} g(t) dt. \quad (2.9)$$

Summing Eq. (2.7) over n and applying the Fourier and Laplace transformations defined above, we obtain through the use of the convolution theorems the matrix equation

$$\underline{\tilde{Q}}^*(\vec{k}, u) = [\underline{1} - \underline{\tilde{\psi}}^*(\vec{k}, u)]^{-1}, \quad (2.10)$$

where the walker is assumed to be initially at the origin $(\vec{S} = 0)$ cell.

The quantity $P_{j j_0}(\vec{S}, t)$ is related to $Q_{j j_0}(\vec{S}, \tau)$ via the aid of the probability $\Gamma_j(\tau)$ that a walker arriving at a point $(\vec{S}, j)$ at $t = 0$ has not changed state in the time interval τ after arrival. Thus

$$P_{j j'}(\vec{S}, t) = \int_0^t \Gamma_j(t - \tau) Q_{j j'}(\vec{S}, \tau) d\tau, \quad (2.11)$$

and [see Eq. (2.6)]

$$\Gamma_j(t) = 1 - \int_0^t \psi_j(\tau) d\tau. \quad (2.12)$$

Performing Laplace and Fourier transformation of Eqs. (2.11) and (2.12) and employing the convolution theorem yields [using (2.10)]

$$\underline{P}^*(\vec{k}, u) = u^{-1}[\underline{1} - \tilde{\underline{\psi}}_d(u)]\,\tilde{\underline{Q}}^*(\vec{k}, u) \qquad (2.13a)$$

$$= u^{-1}[\underline{1} - \tilde{\underline{\psi}}_d(u)][\underline{1} - \tilde{\underline{\psi}}^*(\vec{k}, u)]^{-1}, \qquad (2.23b)$$

where $\tilde{\underline{\psi}}_d(u)$ is the diagonal matrix

$$\tilde{\underline{\psi}}_d(u) = \begin{pmatrix} \tilde{\psi}_1(u) & \cdots & 0 \\ \vdots & & \vdots \\ 0 & \cdots & \tilde{\psi}_m(u) \end{pmatrix}. \qquad (2.14)$$

Equation (2.13) constitutes the solution to our initially stated problem [Eq. (2.2)], and the computation of the probabilities $P_{jj'}(\vec{S}, t)$ given in terms of the inverse Laplace and Fourier transformations of Eq. (2.13) is reduced to quadratures.

Quantities of interest in the investigation of the stochastic motion of particles are moments of the probability distribution and equilibrium probabilities of occupation of states. As we show below, these quantities are derived most readily in terms of the transformed expression $\tilde{P}^*(\vec{k}, u)$ [Eq. (2.13)].

(i) The lth spatial moment of the probability distribution in the αth coordinate direction is defined

as

$$\langle s_\alpha^l(t) \rangle = \sum_{s_\alpha} \sum_{j, j'} s_\alpha^l P_{jj'}(s_\alpha; t) p_{j'}, \qquad (2.15)$$

where p_j is the probability that the walker is initially in state j. Performing an inverse Laplace transformation, Eq. (2.13a) yields

$$\underline{P}^*(\vec{k}, t) = \mathcal{L}^{-1}\left(u^{-1}[\underline{1} - \tilde{\underline{\psi}}_d(u)] \sum_{\vec{S}} e^{-i\vec{k}\cdot\vec{S}} \underline{\tilde{Q}}(\vec{S}, u) \right). \qquad (2.16)$$

Differentiating (2.16) l times with respect to $\vec{k}$ and evaluating the result at $\vec{k} = 0$, we obtain

$$\frac{\partial^l \underline{P}^*(\vec{k}, t)}{\partial \vec{k}^l}\bigg|_{\vec{k}=0} = \mathcal{L}^{-1}\left(u^{-1}[\underline{1} - \tilde{\underline{\psi}}_d(u)] \sum_{\vec{S}} (i\vec{S})^l \underline{\tilde{Q}}(\vec{S}, u) \right)$$

$$= i^l \mathcal{L}^{-1}\left(\sum_{\vec{S}} \vec{S}^l \underline{\tilde{P}}(\vec{S}, u) \right). \qquad (2.17)$$

Comparing (2.17) and (2.15), we observe that

$$\langle S_\alpha^l(t) \rangle = (-i)^l \sum_{j, j'} \frac{\partial^l P_{jj'}^*(\vec{k}, t)}{\partial k_\alpha^l}\bigg|_{\vec{k}=0} p_{j'}. \qquad (2.18)$$

Using (2.16) in (2.18), we obtain the final expression

$$\langle S_\alpha^l(t) \rangle = (-i)^l \sum_{j, j'} \mathcal{L}^{-1}\left(\frac{\partial^l \tilde{Q}_{jj'}^*(\vec{k}, u)}{\partial k_\alpha^l}\bigg|_{\vec{k}=0} u^{-1}[1 - \tilde{\psi}_j(u)] \right) p_{j'}. \qquad (2.19a)$$

In the diffusion limit ($t \to \infty$ and $u \to 0$) the elements of the matrix $\tilde{\underline{Q}}^*$ become independent of j', and since $\sum_{j'} p_{j'} = 1$, the corresponding expression for the moments is given by

$$\langle S_\alpha^l(t \to \infty) \rangle = (-i)^l \sum_j \mathcal{L}^{-1}\left(\lim_{u \to 0} \frac{\partial^l \tilde{Q}_{j}^*(\vec{k}, u)}{\partial k_\alpha^l}\bigg|_{\vec{k}=0} u^{-1}[1 - \tilde{\psi}_j(u)] \right). \qquad (2.19b)$$

When $l = 1$, we obtain the mean distance of motion. The mean and the second moment ($l = 2$) are used in the calculation of the variance

$$\sigma_\alpha^2 \equiv \langle s_\alpha^2 \rangle - \langle s_\alpha \rangle^2. \qquad (2.20)$$

(ii) The equilibrium probability of occupation of the internal state j, $P_{j, \text{eq}}$, is defined by

$$P_{j, \text{eq}} = \lim_{t \to \infty} \sum_m \sum_{\vec{S}} P_{jm}(\vec{S}, t) p_m. \qquad (2.21a)$$

In the Laplace-transform domain, (2.21a) can be written as[32]

$$P_{j, \text{eq}} = \lim_{u \to 0} u \sum_m \sum_{\vec{S}} \tilde{P}_{jm}(\vec{S}, u) p_m. \qquad (2.21b)$$

Since

$$\lim_{\vec{k} \to 0} \tilde{P}_{jm}^*(\vec{k}, u) = \sum_{\vec{S}} \tilde{P}_{jm}(\vec{S}, u),$$

and using Eq. (2.16), we can finally express $P_{j, \text{eq}}$

in (2.21b) as

$$P_{j, \text{eq}} = \lim_{u \to 0} \lim_{k \to 0} \sum_m \tilde{Q}_{jm}^*(\vec{k}, u)[1 - \tilde{\psi}_j(u)] p_m. \qquad (2.22a)$$

In the long-time limit ($t \to \infty$ or, equivalently, $u \to 0$) the elements of the matrix $\tilde{Q}^*(k, u)$ do not depend on m for fixed j, and

$$P_{j, \text{eq}} = \lim_{u \to 0} \lim_{k \to 0} \{\tilde{Q}_{j1}^*(\vec{k}, u)[1 - \tilde{\psi}_j(u)]\}. \qquad (2.22b)$$

We observe from Eqs. (2.19) and (2.22) that the key quantities in calculating the moments of the probability function are derivatives of the function $\tilde{\underline{Q}}^*(\vec{k}, u)$ given in Eq. (2.10). Denoting the determinant of $\tilde{\underline{Q}}^*$ [given in Eq. (2.10)] by Δ and the matrix of cofactors by $\underline{M}$ [the ij element of $\underline{M}$ being $(-1)^{i+j} \times (ji$ cofactor of $\tilde{\underline{Q}}^*)$], we express $\tilde{\underline{Q}}^*$ as

$$\tilde{\underline{Q}}^* = \underline{M}/\Delta. \qquad (2.23)$$

Differentiating (2.23) with respect to $\vec{k}$, we obtain

$$\frac{\partial \tilde{Q}^*(\vec{k}, u)}{\partial \vec{k}}\bigg|_{\vec{k}=0} = -\frac{1}{\Delta^2}\frac{\partial \Delta}{\partial \vec{k}}\underline{M}\bigg|_{\vec{k}=0} + \frac{1}{\Delta}\frac{\partial M}{\partial \vec{k}}\bigg|_{\vec{k}=0} \quad (2.24)$$

$$\frac{\partial^2 \tilde{Q}^*(\vec{k}, u)}{\partial \vec{k}^2}\bigg|_{\vec{k}=0} = \frac{2}{\Delta^3}\left(\frac{\partial \Delta}{\partial \vec{k}}\right)^2 \underline{M}\bigg|_{\vec{k}=0} - \frac{1}{\Delta^2}\frac{\partial^2 \Delta}{\partial \vec{k}^2}\underline{M}\bigg|_{\vec{k}=0}$$

$$-\frac{2}{\Delta^2}\frac{\partial \Delta}{\partial \vec{k}}\frac{\partial M}{\partial \vec{k}}\bigg|_{\vec{k}=0} + \frac{1}{\Delta}\frac{\partial^2 M}{\partial \vec{k}^2}\bigg|_{\vec{k}=0}.$$

$$(2.25)$$

When considering the motion in the diffusion regime (to which the present study is devoted), only those terms in the expressions for the first moment (when a bias is present) and the variance which grow linearly with time are of interest. This brings about a significant simplification, since (as will become evident from the detailed examples in the next section) the only divergent terms in u as $u \to 0$ in the expressions for the position mean and variance are powers of the inverse of Δ [see Eq. (2.23)–(2.25)] which in the limit of $\vec{k} \to 0$ can be written as

$$\lim_{k \to 0}[\Delta(\vec{k}, u)]^{-1} \propto \left(u\sum_{j=1}^{m-1} \lambda_i u^{i-1}\right)^{-1}, \quad (2.26)$$

where m is the number of internal states and the λ's are constants. The evaluation of the moments of the probability distribution involves an inverse Laplace transformation [see Eq. (2.19)] of expressions of the form of Eq. (2.26) [see Eqs. (2.23)–(2.25)]. We utilize now the following relation, known from the theory of Laplace transforms[32]:

$$\frac{1}{\Gamma(r+1)}\int_0^{\infty} t^r e^{-tu}dt = u^{-r-1}, \quad (2.27)$$

where $\Gamma(r)$ is the gamma function. Since we are interested in terms which, subject to an inverse Laplace transformation, yield expressions linear in t (t and u are conjugated Laplace variables; i.e., when $t \to \infty$, the conjugated variable $u \to 0$), only terms which diverge as u^{-2} (in the limit $u \to 0$) will contribute. Terms which behave as t^2, originating from u^{-3} terms in the (Laplace-transformed) expression for the variance [Eq. (2.20)], will always cancel. Contributions to the moments other than those linear in t depend on the initial spatial configuration of the cluster and are either constant (of the order of the lattice spacing) or decay in time and thus can be neglected in the diffusion (long-time) limit.

In concluding this section we note that a formulation equivalent to the continuous-time random walk with internal states discussed above can be given in terms of the generalized master equation[27] (GME)

$$\frac{d\underline{P}(\vec{S}, t)}{dt} = \int_0^t \sum_{\vec{S}} [\underline{\Phi}(\vec{S} - \vec{S}'; \tau)\underline{P}(\vec{S}', t - \tau)$$

$$-\underline{\Phi}(\vec{S}' - \vec{S}, \tau)\underline{P}(\vec{S}, t - \tau)]d\tau, \quad (2.28a)$$

where the elements of $\underline{\Phi}$ are

$$\Phi_{jj'}(\vec{S}, \tau) = \phi_{j'}(\tau)F_{jj'}(\vec{S}, \tau), \quad (2.28b)$$

and F is the function defined in Eq. (2.5), subject to the equivalency conditions

$$\tilde{\phi}^*(\vec{k}, u) = u\tilde{\psi}^*(\vec{k}, u)[\underline{1} - \tilde{\psi}_\alpha(u)]^{-1} \quad (2.29a)$$

and the diagonal matrix $\tilde{\Phi}_d(u)$ given as

$$\tilde{\phi}_d(u) = u\tilde{\psi}_d(u)[\underline{1} - \tilde{\psi}_d(u)]^{-1}. \quad (2.29b)$$

For $\phi_j(\tau) = \delta(\tau)$, the GME [Eq. (2.28a)] becomes the well-known Kolmogorov equation. We choose to work within the continuous-time-random-walk formalism, since it provides a compact framework which can be easily applied to complicated cases. In the following we list the steps involved in calculations using the CTRW with internal-states formalism.

B. Procedure

Step 1. Examine the allowed spatial configurations for the cluster. For each configuration determine the location of the centroid and map the latter onto a lattice. Determine the unit cell of the centroid-random-walk lattice. The centroid may move on a one- or higher-dimensional lattice.

Step 2. Label the allowed transitions between states, within and out of the unit cell.

Step 3. Construct the transition matrix

$$\underline{\psi}(\vec{S}, t) \text{ [Eq. (2.5)]}.$$

Step 4. Perform a discrete Fourier transformation with respect to $\vec{S}$ [see Eq. (2.8)] and a Laplace transformation with respect to t [see Eq. (2.9)] of $\underline{\psi}(\vec{S}, t)$. Denote the transformed matrix by $\tilde{\psi}^*(\vec{k}, u)$.

Step 5. Form the matrix $\tilde{Q}^*$ [see Eq. (2.10)]:

$$\tilde{Q}^* = \underline{M}/\Delta \text{ [Eq. (2.23)]}.$$

Step 6. Calculate the first and second derivatives of $\tilde{Q}^*(\vec{k}, u)$ with respect to $\vec{k}$, and evaluate at $\vec{k} = 0$ [see Eqs. (2.24) and (2.25)].

Step 7. Employing step 6, calculate the moments of the probability distribution of the motion [see Eq. (2.19)]. In this calculation, when performing the inverse Laplace transformation, only terms which contribute in the diffusion limit are retained (see the discussion at the end of Sec. II A). Also, we use $\tilde{Q}^*(\vec{k}, u)$ obtained in step 5 for the evaluation of the equilibrium occupation probabilities [see Eq. (2.22)].

Step 8. The diffusion coefficient (or coefficients

for motion in two dimensions) and detailed balance relations are given as functions of the transition rates. In order to extract information about *individual* transition rates, the above equations are solved yielding expressions for the transition rates in terms of observable quantities: variance of the position, occupation probabilities, and mean position (in the case of experiments employing a bias field).

III. CASE STUDIES OF CLUSTER DIFFUSION

Having described in the previous sections the mathematical model and the analytical procedure for the study of cluster motion on surfaces, we turn in this section to detailed demonstrations of the application of the method. First we discuss the motion of a 3-state dimer in one dimension, followed by a study of the motion of a 3-state dimer in two dimensions.

A. Three- and two-state dimers in one dimension

Following the procedure described in Sec. II B, we construct first the centroid random-walk lattice shown in Fig. 1(c). Next (step 3) we form the matrix $\underline{\psi}(\vec{S}, t)$ [Eq. (2.5)] which contains the probability density functions for the allowed transitions. In constructing the matrix we assume for the waiting-time density function the form

$$\psi_j(t) = \lambda_j \exp(-\lambda_j t), \qquad (3.1)$$

where λ_j is the sum of the transition rates out of state j. For example, the element $\psi_{21}(s - s'; t)$ governing the transition $(s, 1) \to (s', 2)$ is given by

$$F_{21}(s - s'; t)\psi_1(t) = \frac{a\delta_{s-s',0} + \alpha\delta_{s-s',-1}}{a + \alpha} (a + \alpha)e^{-(a+\alpha)t}.$$

The matrix $\underline{\psi}(s, t)$ is given by (in the following we invoke translational invariance)

$$\underline{\psi}(s, t) = \begin{pmatrix} 0 & e^{-Ut}(b\delta_{s,+1} + \beta\delta_{s,0}) & 0 \\ e^{-At}(a\delta_{s,0} + \alpha\delta_{s,-1}) & 0 & e^{-Dt}(d\delta_{s,0} + (\delta)\delta_{s,-1}) \\ 0 & e^{-Ut}(c\delta_{s,1} + \gamma\delta_{s,0}) & 0 \end{pmatrix}, \qquad (3.2)$$

where $A = a + \alpha$, $B = b + \beta$, etc., and $U = B + C$. In the next step (4) we Fourier- and Laplace-transform the matrix given in (3.2), yielding

$$\underline{\tilde{\psi}}^*(k, u) = \begin{pmatrix} 0 & (U+u)^{-1}(be^{+ik} + \beta) & 0 \\ (A+u)^{-1}(a + \alpha e^{-ik}) & 0 & (D+u)^{-1}(d + \delta e^{-ik}) \\ 0 & (U+u)^{-1}(ce^{ik} + \gamma) & 0 \end{pmatrix}. \qquad (3.3)$$

We now construct (step 5) the matrix $\underline{Q}^*(k, u) = \underline{M}/\Delta$, yielding

$$\underline{M}(k, u) = \begin{pmatrix} 1 - (\delta e^{-ik} + d)(ce^{ik} + \gamma)/(B + C + u)(D + u) & (be^{ik} + \beta)/(B+C) & (be^{ik} + \beta)(d + \delta e^{-ik})/(B + C + u)(D + u) \\ (\alpha e^{-ik} + a)/(A + u) & 1 & (d + \delta e^{-ik})/(D + u) \\ (\alpha e^{-ik} + a)(ce^{ik} + \gamma)/(B + C + u)(A+u) & (ce^{ik} + \gamma)/(B + C) & 1 - (be^{ik} + \beta)(\alpha e^{-ik} + a)/(A + u)(B + C + u) \end{pmatrix}, \qquad (3.4)$$

and [see Eq. (2.26)]

$$\lim_{k \to 0} [\Delta(k, u)]^{-1} = (A + u)(D + u)(U + u) [(CA + BD + AD)u + (A + B + C + D)u^2 + u^3]^{-1}, \qquad (3.5a)$$

which diverges as u^{-1} when $u \to 0$. Also,

$$\lim_{\substack{k \to 0 \\ u \to 0}} \frac{\partial \Delta(k, u)}{\partial k} = -i[(cd - \gamma\delta)A + (ab - \alpha\beta)D]$$

$$\times [AD(B + C)]^{-1} \qquad (3.5b)$$

and

$$\lim_{\substack{k \to 0 \\ u \to 0}} \frac{\partial^2 \Delta(k, u)}{\partial k^2} = [(cd + \gamma\delta)A + (ab + \alpha\beta)D]$$

$$\times [AD(B + C)]^{-1}. \qquad (3.5c)$$

From Eq. (3.4) we obtain

$$\underline{M}(k = 0, u = 0) = \begin{pmatrix} B/(B+C) & B/(B+C) & B/(B+C) \\ 1 & 1 & 1 \\ C/(B+C) & C/(B+C) & C/(B+C) \end{pmatrix}. \qquad (3.6)$$

Note that the elements in each row of the matrix in (3.6) are equal. This implies that in the diffusion limit the probability $P_{jj'}(s, t)$ [see Eq. (2.11)] is in-

deed independent of the initial state j'. On the other hand, the limiting expression of the derivative of the matrix

$$\frac{\partial M}{\partial k}\bigg|_{k=u=0} = i \begin{pmatrix} -(dc - \delta\gamma)/(B+C)D & b/(B+C) & (bd - \delta\beta)/(B+C)D \\ -\alpha/A & 0 & -\delta/D \\ (ac - \alpha\gamma)/(B+C)A & c/(B+C) & -(ab - \alpha\beta)/(B+C)A \end{pmatrix} \quad (3.7)$$

would yield results which depend on the initial configuration. Such terms should not contribute in the diffusion limit. Explicit calculations show that these terms cancel each other in the complete expression for the position variance and mean or are negligible compared to the terms which do not depend on initial conditions. Consequently, terms such as $\Delta^{-1}\partial M/\partial k$, $2\Delta^{-2}(\partial\Delta/\partial k)(\partial M/\partial k)$, and $\Delta^{-1}(\partial^2 M/\partial k^2)$ [see Eqs. (2.24) and (2.25)] will not contribute to the moments. Finally, we form the waiting-time matrix [see Eq. (2.19)]

$$\underline{\bar{W}}(u) \equiv u^{-1}[\underline{1} - \underline{\bar{\psi}}_d(u)] . \quad (3.8a)$$

The ith element $\bar{\psi}_i(u)$ of the diagonal matrix $\underline{\bar{\psi}}_d(u)$ is calculated by considering the probability density for leaving site i, independent of which configuration the cluster takes when state i is vacated. We obtain

$$\underline{\bar{W}}(u) = \begin{pmatrix} (A+u)^{-1} & 0 & 0 \\ 0 & (B+C+u)^{-1} & 0 \\ 0 & 0 & (D+u)^{-1} \end{pmatrix} . \quad (3.8b)$$

Having calculated the ingredients which enter the expressions for the moments and equilibrium probabilities, we turn now to a derivation of the final expressions for these quantities.

The first moment (mean position) is calculated from Eq. (2.19b) with $l = 1$:

$$\lim_{t\to\infty} \langle s(t)\rangle_3 \equiv \langle l(t)\rangle_3$$
$$= -i \sum_j \mathcal{L}^{-1}\left[\lim_{u\to 0}\left(\frac{\partial \bar{Q}_{ji}^*(k,u)}{\partial k}\right)_{k=0} \bar{W}_{jj}(u)\right] , \quad (3.8c)$$

where the matrix $\bar{W}(u)$ is defined in Eq. (3.8a) and $\langle l(t)\rangle_3$ denotes the long-time limit of the mean position for the 3-state dimer. Using Eqs. (2.24), (3.5a), (3.5b), and (3.6), we obtain

$$\langle l(t)\rangle_3 = \frac{A(cd - \gamma\delta) + D(ab - \alpha\beta)}{AC + BD + AD} t . \quad (3.9)$$

In the above expression we have omitted an additive constant term, dependent on the initial configuration (of the order of a lattice spacing) on the right-hand side of Eq. (3.9), whose contribution is negligible for sufficiently long times.

Calculation of the variance [Eq. (2.20)] involves the second moment $\langle s^2\rangle$. From Eq. (2.19b) it is seen that the second derivative of $\bar{Q}^*(k,u)$ with respect to k, evaluated at $k = 0$ in the limit of $u \to 0$, has to be calculated. As is seen from Eq. (2.25), the first term involves a Δ^{-3} contribution. It is observed from Eq. (3.5a) that in the $u \to 0$ limit two additive divergent contributions to this term occur. One diverges as u^{-3} and the other as u^{-2}, since the other factors in the first term of Eq. (2.25) do not diverge as $u \to 0$ [see Eqs. (3.5b) and (3.6)]; this term, upon a Laplace inversion, yields contributions which are proportional to t^2 and t, respectively. The t^2 contribution is canceled by $-\langle l(t)\rangle_3^2$ [Eq. (3.9)]. Other terms which depend on initial conditions or are independent of time cancel each other or are neglected in the limit of sufficiently long times [for a proper cancellation of terms the constant term in Eq. (3.9) is to be included]. Finally, we obtain for the variance in position of the 3-state dimer

$$t^{-1}\sigma_3^2(t) = Z^{-1}[A(cd + \gamma\delta) + D(ab + \alpha\beta)]$$
$$- 2t^{-1}\langle l(t)\rangle_3 Z^{-2}[(A^2 + AB - BD)(cd - \gamma\delta)$$
$$+ (D^2 + DC - AC)(ab - \alpha\beta)] , \quad (3.10a)$$

where

$$Z = AC + BD + AD , \quad (3.10b)$$

and $\langle l(t)\rangle_3$ is given by Eq. (3.9). Examination of Eq. (3.9) reveals that indeed in the case of no bias $(a = \alpha, \; b = \beta, \; c = \gamma, \; \text{and} \; d = \delta)$ the mean position vanishes as required. For this case of a bias-free experiment the variance is given by

$$t^{-1}\sigma_3^2(t) = ad(c + b)z^{-1} , \quad (3.11a)$$
$$z = ac + bd + ad . \quad (3.11b)$$

Using the expressions for the variance and mean for the 3-state dimer, we can now recover the corresponding expressions for a 2-state dimer by disallowing the transition to the third state, i.e., in the limit of vanishing transition rates c and γ. From Eq. (3.9) we obtain for the mean position of a 2-state dimer (under a bias field)

$$\langle l(t)\rangle_2 = \frac{ab - \alpha\beta}{A + B} t , \quad (3.12)$$

and for the variance, Eqs. (3.10) yield

$$\sigma_2^2(t) = \left(\frac{ab+\alpha\beta}{A+B} - 2\frac{(ab-\alpha\beta)^2}{(A+B)^3}\right)t. \tag{3.13}$$

Again, if no bias is present, $\langle l(t)\rangle_2$ vanishes and

$$\sigma_2^2(t) = \frac{ab}{a+b}t. \tag{3.14}$$

The last expression was previously derived by Reed and Ehrlich[26] starting from a Kolmogorov master equation. The factor-of-4 difference between Eq. (3.14) and Eq. (25) in Ref. 26 is due to different definitions of the random-walk unit cell.

Finally, we derive the expressions for the equilibrium occupation probabilities of states. Using Eqs. (2.23), (3.5a), (3.6), and (3.8b) (multiplied by u) in Eq. (2.22b), we obtain in the long-time limit

$$P_{1,\mathrm{eq}} = BDZ^{-1}, \tag{3.15a}$$

$$P_{2,\mathrm{eq}} = ADZ^{-1}, \tag{3.15b}$$

$$P_{3,\mathrm{eq}} = ACZ^{-1}, \tag{3.15c}$$

where Z is defined in Eq. (3.10b). Defining the relative state population factors (detailed balance relations) as $R_{ij} = P_{i,\mathrm{eq}}/P_{j,\mathrm{eq}}$, we obtain two independent relationships,

$$R_{12} = B/A, \quad R_{23} = D/C. \tag{3.16}$$

This completes the derivation of quantities describing the motion of a 3-state dimer in one dimension. Prior to solving the equations for the individual transition rates between the states, we discuss in the following the motion of a 3-state dimer in two dimensions.

B. 3-state dimer in two dimensions

The first two steps of the solution procedure (Sec. IIB) are contained in Figs. 2(a) and 2(b). Next (step 3), we construct the transition matrix

$$\underline{\psi}(\vec{S},t) = \begin{pmatrix} 0 & e^{-(B+C)t}(b\delta_{xy,10}+\beta\delta_{xy,00}) & 0 \\ e^{-At}(a\delta_{xy,00}+\alpha\delta_{xy,-10}) & 0 & e^{-Dt}[d\delta_{xy,01}+(\delta)\delta_{xy,00}] \\ 0 & e^{-(B+C)t}(c\delta_{xy,00}+\gamma\delta_{xy,0-1}) & 0 \end{pmatrix}. \tag{3.17}$$

Performing (step 4) the Fourier and Laplace transformations of Eq. (3.17), we construct the matrix $\underline{Q}^* = \underline{M}/\Delta$ (step 5), yielding

$$\underline{M}(\vec{k},u) = \begin{pmatrix} 1 - T^{-1}(\gamma e^{-ik_y}+c)(de^{ik_y}+\delta) & S^{-1}(be^{ik_x}+\beta) & T^{-1}(be^{ik_x}+\beta)(de^{ik_y}+\delta) \\ (\alpha e^{-ik_x}+a)/(A+u) & 1 & (de^{ik_y}+\delta)/(D+u) \\ T^{-1}(be^{-ik_x}+\beta)(de^{-ik_y}+\delta) & S^{-1}(\gamma e^{-ik_y}+c) & 1-R^{-1}(be^{ik_x}+\beta)(\alpha e^{-ik_x}+a) \end{pmatrix}, \tag{3.18a}$$

where

$$T = (D+u)(B+C+u), \tag{3.18b}$$

$$S = B+C+u, \tag{3.18c}$$

$$R = (A+u)(B+C+u), \tag{3.18d}$$

and

$$\Delta(\vec{k},u) = 1 - T^{-1}(\gamma e^{-ik_y}+c)(de^{ik_y}+\delta)$$
$$-R^{-1}(\alpha e^{-ik_x}+a)(be^{ik_x}+\beta). \tag{3.19}$$

Employing the above expressions in the procedure described in Sec. IIB, we obtain after some tedious algebraic manipulations the following expressions for the x Cartesian components:

$$\langle l_x(t)\rangle = Z^{-1}D(ab-\alpha\beta)t \tag{3.20}$$

and

$$t^{-1}\sigma_x^2(t) = Z^{-1}[D(ab+\alpha\beta) - 2t^{-2}\langle l_x(t)\rangle^2$$
$$\times D^{-1}(D^2+DC-AC)], \tag{3.21}$$

where Z is given by Eq. (3.10b). From the symmetry in Fig. 2 we obtain the expressions for the y Cartesian components

$$\langle l_y(t)\rangle = Z^{-1}A(cd-\gamma\delta)t \tag{3.22}$$

and

$$t^{-1}\sigma_y^2(t) = Z^{-1}[A(cd+\gamma\delta) - 2t^{-2}\langle l_y(t)\rangle^2$$
$$\times A^{-1}(A^2+AB-BD)]. \tag{3.23}$$

The corresponding expressions in the absence of a bias field are obtained by setting $a=\alpha$, $b=\beta$, $c=\gamma$, and $d=\delta$, yielding

$$t^{-1}\sigma_x^2(t) = abdz^{-1}, \tag{3.24}$$

$$t^{-1}\sigma_y^2(t) = acdz^{-1}, \tag{3.25}$$

where z is given by Eq. (3.11b). We also note that if transitions into the states propagating in the y direction are prohibited ($c,\gamma\to0$; $\delta,d\to\infty$), the above results reduce to the corresponding ones for the motion of a 2-state dimer in one dimension.

The equilibrium population of states are given by

$$P_{1,\text{eq}} = Z^{-1}BD ,\qquad\qquad (3.26\text{a})$$

$$P_{2,\text{eq}} = Z^{-1}AD ,\qquad\qquad (3.26\text{b})$$

$$P_{3,\text{eq}} = Z^{-1}AC .\qquad\qquad (3.26\text{c})$$

The detailed balance relations for this case are

$$R_{12} = B/A ,\quad R_{23} = D/C .\qquad\qquad (3.27)$$

IV. TRANSITION RATES

As we discussed above, in our model the migration of clusters of atoms on surfaces proceeds via transitions between several configurations of the cluster. This view is supported by the FIM observations discussed in Sec. I. The allowed configurations are dictated by the topology of the substrate lattice on which the migration occurs, the potential and dynamical characteristics of the lattice, the energetics and dynamics of the interaction between the atoms of the cluster and the underlying surface, and the intercluster interactions. The parameters which characterize the transitions between the various cluster configurations, and hence the motion of the cluster, are a consequence of the above-mentioned factors. Thus, the determination of the parameters (activation energies and frequency factors) characterizing the individual transitions would be of fundamental importance for the study of the interaction and migration mechanisms. Analytical procedures which would allow the determination of these parameters from the analysis of FIM data are described below.[33] In this section we utilize the expressions derived in Sec. III, in order to express the individual transition rates in terms of measurable quantities. When the motion of a *single particle* is of diffusional character (a classification which depends mainly on the temperature of the experiment[8(c)]), the results are customarily analyzed in terms of the diffusion coefficient D, which is related to the variance in position $\sigma^2(t)$ (in the long-time limit) as[34]

$$D = \lim_{t \to \infty} \frac{\sigma^2(t)}{2\epsilon t} ,\qquad\qquad (4.1)$$

where ϵ is the dimensionality of the random walk ($\epsilon = 1$ or 2 for surface diffusion). The diffusion coefficient is assumed to be given by an activated form of the Arrhenius type:

$$D = D_0 \exp(-E_m^{\ddagger}/kT) ,\qquad\qquad (4.2)$$

where $E_m^{\ddagger}$ is the magnitude of the activation barrier and D_0 is a prefactor. For an unrestricted random walk on a lattice of spacing l the variance is related (in the long-time limit) to the transition (jump) rate ξ via (in the following we omit the limit

symbol)

$$\sigma^2(t) = \xi t l^2 \quad (= 2\epsilon D t) ,\qquad\qquad (4.3)$$

and ξ assumes an activated-process form

$$\xi = \nu \exp(-E^{\ddagger}/kT) ,\qquad\qquad (4.4)$$

where ν is called a frequency factor and $E^{\ddagger}$ the activation energy of the transition. Thus the diffusion coefficient (or the variance of the displacement) and the transition rates are related to each other.

Our objective is to derive relations between the transition rates of cluster configurations and observables such as moments of the displacement and equilibrium occupation probabilities of states. In the following we will use the following form for the transition rates[11]:

$$a = \nu_a \exp\{-[E_a - g(v)]/kT\} ,\qquad\qquad (4.5\text{a})$$

$$\alpha = \nu_a \exp\{-[E_a + g(v)]/kT\} ,\quad \text{etc.},\qquad (4.5\text{b})$$

where ν_a is the frequency factor of the transition, E_a the activation energy, and v the applied bias voltage (we assume the forward direction, characterized by a, in the direction of the applied field). The function $g(v)$ describes the effect of the applied field on the activation energy. In most applications

$$g(v) = \mu v^\theta ,\qquad\qquad (4.6)$$

where μ and θ are empirical constants.

In general, when the motion of a cluster is characterized by n transition rates between its configurations, it is necessary to find n independent relations in order to achieve a unique determination of all the rates. In the case of m allowed cluster configurations one can obtain $m - 1$ independent detailed balance relationships: $R_{12}, R_{13}, \ldots, R_{1m}$. The remaining $n - m + 1$ relationships required for complete determination must be obtained from the cumulants of the displacement probability distribution of the cluster, i.e., $\langle l(t) \rangle$, $\sigma^2(t)$, and higher cumulants, if they can be determined from the data. In the event that more relationships are at our disposal than the number of transition rates n, there are several ways in which we can choose the n necessary relationships, allowing for consistency checks on the results derived via different alternatives.

A. 3- and 2-state dimers in one dimension

As a first example we consider the 3-state dimer discussed in Sec. III A. Since the forward and backward transition rates are related to each other [Eqs. (4.5)], we need to determine the four rates a, b, c, and d. Detailed balance between the 3 states yields two relationships [Eq. (3.16)]. The

other two relations are given by the expressions for the mean and variance. Since the mean vanishes in the absence of a bias, the above implies that in this case the application of a bias field is *necessary* for a complete determination of the four rates. Substituting Eqs. (4.5) and the corresponding ones for the other rates in Eqs. (3.9) and (3.10), we obtain the following expressions for the mean and variance, respectively:

$$t^{-1}\langle l(t)\rangle_3 = ad(b+c)z^{-1}F_1(g(v)/kT),\qquad(4.7a)$$

where

$$F_1(g(v)/kT) = 2\sinh[g(v)/kT]\exp[-g(v)/kT],$$
$$(4.7b)$$

and

$$t^{-1}\sigma_3^2(t) = t^{-1}\langle l(t)\rangle_3 F_1^{-1}(g(v)/kT)F_2(g(v)/kT)$$
$$- 2t^{-1}z^{-2}\langle l(t)\rangle_3[(d^2+dc-ac)(ab-\alpha\beta)$$
$$+ (a^2+ab-bd)(cd-\gamma\delta)],\qquad(4.8a)$$

where

$$F_2(g(v)/kT) = \frac{1+\exp[-4g(v)/kT]}{1+\exp[-2g(v)/kT]}\qquad(4.8b)$$

and

$$F_3(g(v)/kT) = \frac{1-\exp[-4g(v)/kT]}{\{1+\exp[-2g(v)/kT]\}^2}.\qquad(4.8c)$$

Together with the two detailed balance relations $R_{12}=b/a$ and $R_{23}=d/c$, the above relations allow us to solve for the individual transition rates:

$$a = 2^{-1}[-\lambda_1-(\lambda_1^2-4\lambda_2)^{1/2}],\qquad(4.9a)$$

$$b = aR_{12},\qquad(4.9b)$$

$$c = H_1-b,\qquad(4.9c)$$

$$d = cR_{23},\qquad(4.9d)$$

where

$$\lambda_1 = -H_1R_{23}(H_3+2R_{12}R_{23})Y^{-1},\qquad(4.10a)$$

$$\lambda_2 = H_1^2R_{23}^2Y^{-1},\qquad(4.10b)$$

and

$$H_1 = t^{-1}\langle l(t)\rangle_3(1+R_{12}+R_{23}^{-1}),\qquad(4.11a)$$

$$H_2 = t^{-1}[\sigma_3^2(t)-\langle l(t)\rangle_3 F_1^{-1}F_2](1+R_{23}+R_{12}R_{23})$$
$$\times[2t^{-1}\langle l(t)\rangle_3 F_3]^{-1},\qquad(4.11b)$$

$$H_3 = (R_{12}+R_{23}^{-1}+2R_{12}R_{23}^{-1}+H_2)R_{23}R_{12}^{-1},\qquad(4.11c)$$

$$Y = 1+R_{12}R_{23}H_3+R_{12}^2R_{23}^2.\qquad(4.11d)$$

Thus, from the measurements of $\langle l(t)\rangle_3, \sigma_3^2(t)$, $R_{12}(T)$, $R_{23}(T)$, at time t and bias voltage v, versus T, the transition rates can be found. For example, from Eq. (4.9a)

$$\nu_a\exp(-E_a/kT) = 2^{-1}[-\lambda_1-(\lambda_1^2-4\lambda_2)^{1/2}]$$
$$\times\exp[-g(v)/kT].\qquad(4.12)$$

Plotting the logarithm of the right-hand side of Eq. (4.12) vs $(kT)^{-1}$ yields $-E_a$ as the slope and $\ln\nu_a$ as the intercept. Similar plots of b, c, and d using Eqs. (4.9b)–(4.9d) yield E_b, ν_b, E_c, ν_c, and E_d, ν_d.

The situation simplifies considerably when the most extended state (state 3) of the dimer is prohibited, i.e., for a 2-state dimer. In this case

$$\nu_a\exp(-E_a/kT) = t^{-1}\langle l(t)\rangle_2 f_2(g(v)/kT)$$
$$\times[1+R_{12}^{-1}(T)],\qquad(4.13a)$$

where

$$f(g(v)/kT) = 2^{-1}\operatorname{csch}[g(v)/kT]\qquad(4.13b)$$

and

$$\nu_b\exp(-E_b/kT) = aR_{12}^{-1}.\qquad(4.14)$$

Expressions for a and b can be derived in terms of $\sigma_2^2(t)$ rather than $\langle l(t)\rangle_2$. However, we suggest the use of Eqs. (4.13) and (4.14), since the statistical error involved in the measurement of the mean is smaller than for the variance. For the 2-state dimer in the absence of an applied bias field we obtain

$$a \equiv \nu_a\exp(-Ea/kT) = t^{-1}\sigma_2^2(t)[1+R_{12}(T)],\quad(4.15a)$$

$$b \equiv \nu_b\exp(-Eb/kT) = t^{-1}\sigma_2^2(t)[1+R_{12}^{-1}(T)]$$
$$= aR_{12}^{-1}(T).\qquad(4.15b)$$

These are the relations employed by Stolt *et al.*[22] in their analysis of the diffusion of Re dimers on W(211). Equations (4.13)–(4.15) provide two alternative ways for the determination of the transition rates a and b.

It is obvious from the above examples that *cluster diffusion cannot be described by a single Arrhenius relationship*. Note that although a semilog plot of the latter relationship would appear to be almost a straight line in the typical temperature range of the experiments, its slope and intercept *are not simply related* to the parameters characterizing the transitions between the states.[11]

B. 3-state dimer in two dimensions

We turn in this section to an exposition of the results for the transition rates of a 3-state dimer moving in two dimensions (see Sec. III B). In this case, there are four independent transition rates a, b, c, and d. The detailed balance relations $R_{12}(T) = b/a$ and $R_{23}(T) = d/c$ have to be augmented by two additional relationships to allow a complete determination of the rates. We have derived in Sec. III B expressions for the Cartesian components of the mean and variance [see Eqs. (3.20)–(3.23) for

the biased and (3.24) and (3.25) for the bias-free cases, respectively], $\langle l_x(t)\rangle,\ \langle l_y(t)\rangle,\ \sigma_x^2(t),$ and $\sigma_y^2(t)$. In general, there are 15 alternative ways in which to choose the four relationships from the two detailed balance and four mean and variance equations. In the following we give the results for three of the alternative choices. First, we substitute the forms given in Eqs. (4.5) for the transition rates in Eqs. (3.20)–(3.23), yielding

$$t^{-1}\langle l_x(t)\rangle = z^{-1}abd\,F_1(g(v)/kT),\qquad(4.16a)$$

$$t^{-1}\langle l_y(t)\rangle = z^{-1}acd\,F_1(g(v)/kT),\qquad(4.16b)$$

$$t^{-1}\sigma_x^2(t) = t^{-1}\langle l_x(t)\rangle[F_1(g(v)/kT)]^{-1}$$

$$F_2(g(v)/kT) - 2t^{-2}z^{-1}\langle l_x(t)\rangle^2$$

$$\times\,F_3(g(v)/kT)(c+d-ac/d),\qquad(4.16c)$$

$$t^{-1}\sigma_y^2(t) = t^{-1}\langle l_y(t)\rangle[F_1(g(v)/kT)]^{-1}$$

$$\times F_2(g(v)/kT) - 2t^{-2}z^{-1}\langle l_y(t)\rangle^2$$

$$\times F_3(g(v)/kT)(a+b-bd/a),\qquad(4.16d)$$

where $F_1,\ F_2,$ and F_3 are defined in Eqs. (4.8a), (4.8b), and (4.8c), respectively, and $z = ac + bd + ad$.

The three alternatives which we present are:

(i) Bias-free motion. From Eqs. (3.24) and (3.25) we obtain

$$\sigma_x^2(t)/\sigma_y^2(t) = b/c\ .\qquad(4.17)$$

Combined with the two detailed balance relation, we get

$$b = t^{-1}\sigma_x^2(t)[1 + R_{12}(T) + R_{23}^{-1}(T)]F_2^{-1}\ ,\qquad(4.18a)$$

$$a = bR_{12}^{-1}(T)\ ,\qquad(4.18b)$$

$$c = b[\sigma_y^2(t)/\sigma_x^2(t)]\ ,\qquad(4.18c)$$

$$d = cR_{23}(T)\ ,\qquad(4.18d)$$

from which semilogarithmic plots of the right-hand side versus $(kT)^{-1}$ yield the individual activation energies and frequency factors.

(ii) Motion under an applied bias in the x direction, i.e., $\langle l_y(t)\rangle = 0$ and $\langle l_x(t)\rangle \neq 0$. Employing Eqs. (4.16) and the detailed balance relations, we obtain

$$b = t^{-1}[F_1(g(v)/kT)]^{-1}\langle l_x(t)\rangle$$

$$\times[1 + R_{12}(T) + R_{23}^{-1}(T)],\qquad(4.19a)$$

$$a = bR_{12}^{-1}(T)\ ,\qquad(4.19b)$$

$$d = 2at^{-2}\langle l_x(t)\rangle^2\,F_3(g(v)/kT)$$

$$\times\{2t^{-2}\langle l_x(t)\rangle^2\,F_3(g(v)/kT)(1 + R_{23})$$

$$+[\sigma_x^2(t) - \langle l_x(t)\rangle F_1^{-1}(g(v)/kT)\,F_2(g(v)/kT)$$

$$\times at^{-1}(1 + R_{23} + R_{12}R_{23})]\}\ ,\qquad(4.19c)$$

$$c = dR_{23}^{-1}(T).\qquad(4.19d)$$

(iii) Motion under the influence of a bias field applied in an arbitrary direction such that both $\langle l_x(t)\rangle$ and $\langle l_y(t)\rangle$ do not vanish. Here

$$b = t^{-1}[F_1(g(v)/kT)]^{-1}\langle l_x(t)\rangle$$

$$\times[1 + R_{12}(T) + R_{23}^{-1}(T)],\qquad(4.20a)$$

$$a = bR_{12}^{-1}(T)\ ,\qquad(4.20b)$$

$$d = t^{-1}[F_1(g(v)/kT)]^{-1}\langle l_y(t)\rangle$$

$$\times[1 + R_{12}(T)R_{23}(T) + R_{23}]\ ,\qquad(4.20c)$$

$$c = dR_{23}^{-1}(T)\ .\qquad(4.20d)$$

As we discussed before, analyzing the data via different alternative choices provides a consistency test of the analysis. In addition, from the comparison of results obtained from the analysis of biased and bias-free experiments, the effect of external field on the transition rates[23, 35] [see Eqs. (4.5) and (4.6)] could be investigated.

V. DIFFUSION ON DEFECTIVE LATTICES

While the migration of atoms and atomic clusters on crystalline surfaces in the presence of defects is a broad subject which will be dealt with in detail elsewhere,[36] we outline in this section an extension of the method described in Secs. II and III and demonstrate the effect of periodically situated defects on the diffusion of a single particle on a fourfold-coordinated surface net.

Consider first the motion of a particle on a square net (see Fig. 3) with equal jump probabilities of $\frac{1}{4}$ and equal rates in all directions. For this case, in the long-time limit

$$\sigma_x^2(t) = \sigma_y^2(t) = 2at\qquad(5.1)$$

in units of the square of the unit-cell length, l^2. The waiting-time probability density [see Eq. (3.1)] of leaving any site is (one site in each unit cell)

$$\psi(t) = 4a\exp(-4at)\ .\qquad(5.2)$$

Suppose that we replace in a periodic fashion 25% of the net sites by totally reflecting sites. The corresponding random-walk lattice is identical to the one shown in Fig. 2(b), with $a = \alpha,\ b = \beta,$ etc. Consequently, the corresponding expressions are derived from Eqs. (3.21) and (3.23), yielding

$$t^{-1}\sigma_x^2(t) = 4abd/(ac + ad + bd)\ ,\qquad(5.3a)$$

$$t^{-1}\sigma_y^2(t) = 4acd/(ac + ad + bd).\qquad(5.3b)$$

The factor of 4 in the above equations enters because the length of the unit cell is now twice that of the one given in each direction in Fig. 2(b). With the replacement of $a \to 2a,\ b \to a,\ c \to a,$ and

$d \to 2a$ in Fig. 2(b) [i.e., the waiting-time distribution given by Eq. (5.2)] we obtain from Eqs. (5.3)

$$\sigma_x^2(t) = \sigma_y^2(t) = 2at, \tag{5.4}$$

which is identical to the result for diffusion on the same lattice with no defects (i.e., all sites allowed for the walker; see Fig. 3). This identity is the result of the choice of transition rates in the above, which does not account for the time delay caused by multiple reflections. We can account for such a time delay by observing that, owing to the existence of a defect, as shown in Fig. 4, the rates of leaving states 1 and 3 (which are the first nearest neighbors to the defect site) to site 2 are effectively lowered, since the migrating particle attempts also to achieve state 4, which is excluded from it, and thus is reflected back to the original site (the time delay being the time spent by the particle in attempting these "futile" transitions). For this purpose we replace the original rates of leaving sites 1 and 3 by a rate $2\omega < 4a$, yielding [from Eqs. (5.3)]

$$\sigma_x^2(t) = \sigma_y^2(t) = 4ta/(1 + 2a/\omega) < 2at. \tag{5.5}$$

The inequality in the above equation reflects a lowering of the diffusion constant for motion on the modified defective lattice. We may calculate the modified rate ω by considering the following model. The rates for leaving sites 1, 2, and 3 are all given by $4a$. However, upon attempting transitions from states 1 (or 3) towards the defect, the particle is reflected back to the original state with probability $2q$ (what we call a "futile" walk) and thus achieves state 2 with probability $2p = 1 - 2q$. Thus, if the particle starting at site 1 (or 3) suffers one reflection before it leaves the state toward state 2, its effective transition rate (contributing to its nonzero displacement on the lattice) is $2a$. Such an event occurs with a probability $(2p)(2q)$. Continuing this line of reason, taking into account all reflections before leaving, we find that the effective total transition rate out of state 1 (or 3) is given by

$$2\omega = \sum_{n=1}^{\infty} \frac{4a}{n} (2q)^{n-1} 2p = -4a \frac{p}{q} \ln(2p) < 4a. \tag{5.6}$$

As an example, assume $p = q = 0.25$, yielding from Eq. (5.6)

$$2\omega = -4a \ln 2 \sim 2.76a. \tag{5.7}$$

With this value for 2ω, we obtain from (5.5)

$$\sigma_x^2(t) = \sigma_y^2(t) = 1.64at, \tag{5.8}$$

i.e., an effective ~18% reduction from the $2at$ value, corresponding to the unmodified defective
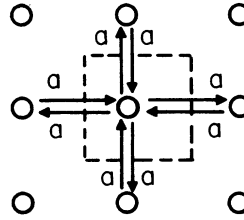

FIG. 3. Random-walk lattice for a single particle in two dimensions. The total rate for leaving any site is $4a$. The unit-cell is designated by dashed lines.

lattice. The variation in the variance for other values of p and q is shown in Fig. 5. As $p/q \to 0$, i.e., when the probability of going towards the defect, q, is larger than the probability of going towards a normal lattice site, the variance approaches zero, since the particle spends its time on futile walks. As $p/q \to \infty$, i.e., when the probability of going to a normal site, p, is larger than the probability of going to a defect site, q, the variance approaches $2at$, which is the value derived for the ideal lattice or a 25% periodic defective lattice (when no account is taken of the time wasted by futile walks).

Until now we considered total reflection from the defect. We can generalize these results by further characterization of the defect site. We introduce the parameter T, such that the particle leaves the defect site (state 4) with probability T; i.e., the probability of the particle to be trapped at the de-
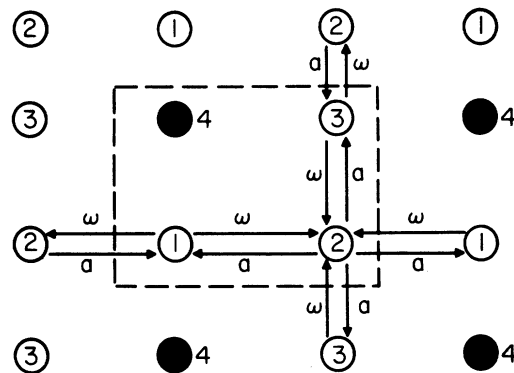

FIG. 4. Random-walk lattice for a single particle in two dimensions, with 25% of the sites replaced periodically by totally reflecting sites (filled circles). The reflecting sites, designated as state 4, form a 2×2 periodic superstructure with respect to the perfect lattice (empty circles). The unit cell used in the random-walk description is denoted by dashed lines. The rate of leaving state 2 (whose nearest neighbors are perfect lattice sites) is denoted by a and the one corresponding to leaving states 1 or 3 (who have reflecting defect neighbors) is denoted by ω [see Eq. (5.6)]. The probability of leaving state 2 is $\frac{1}{4}$ in each direction. The probability of leaving state 1 or 3 towards state 2 is p, and toward a defect site q, such that $2p + 2q = 1$.

fect site is $1 - T$. Thus the parameter T serves to characterize the defect; for $T = 0$ it is totally absorbing and for $T = 1$ totally reflecting. The random-walk lattice and associated rates and probabilities are shown in Fig. 6. We denote the total

transition rates from sites 1 and 3 by $4c$, transition from state 2 by $4a$, and transition from the defect state 4 by $4b$. In accordance with our procedure (Sec. II B) we construct first the transition matrix

$$
\psi(\bar{\mathbf{S}}, t) =
\begin{bmatrix}
0 & ae^{-4at}(\delta_{xy,\,00} + \delta_{xy,\,10}) & 0 & Tbe^{-4bt}(\delta_{xy,\,00} + \delta_{xy,\,01}) \\
4pce^{-4ct}(\delta_{xy,\,00} + \delta_{xy,\,-10}) & 0 & 4pce^{-4ct}(\delta_{xy,\,00} + \delta_{xy,\,01}) & 0 \\
0 & ae^{-4at}(\delta_{xy,\,00} + \delta_{xy,\,0-1}) & 0 & Tbe^{-4bt}(\delta_{xy,\,00} + \delta_{xy,\,-10}) \\
4qce^{-4ct}(\delta_{xy,\,00} + \delta_{xy,\,0-1}) & 0 & 4qce^{-4ct}(\delta_{xy,\,00} + \delta_{xy,\,10}) & (1-T)\delta_{xy,\,00}
\end{bmatrix}
$$

In comparing the present case with that of the motion of an atom on an ideal lattice, it should be noted that the dimension of the unit cell in the present case is twice as large in the x and y directions as in the latter case. Employing our procedure in the manner demonstrated in the previous sections, we obtain in the long-time limit the following expressions for the variance of the displacement:

$$\sigma_x^2(t) = \sigma_y^2(t) = 4Ta^2b^2c^2(T/c + 2pT/a + 2pT/a + 2q/b)$$
$$\times [2qac + bT(a + 2pc)]^{-2}t. \tag{5.10}$$

FIG. 5. Variation of the variance σ_α^2 ($\alpha = x, y$) in units of $2at$, for motion on the lattice shown in Fig. 4, as a function of p/q. Note that the perfect lattice variance is $2at$. As p/q becomes large (i.e., the probability of going towards a defect site is smaller than the probability of migrating to a normal site), σ_α^2 approaches the perfect lattice variance.

The result for the motion on an ideal lattice ($2at$) is recovered from Eq. (5.10) by setting $a = b = c$ and $T = 1$. Note that the limit is obtained for arbitrary choices of p and q, subject to the normalization $2p + 2q = 1$.

In the strong-absorption limit T approaches zero and

$$\lim_{T \to 0} \sigma_{x,y}^2(t) = \frac{2Tb}{q} t. \tag{5.11}$$

The same limiting result is obtained when the particle resides (on the average) at the defect site for times longer than its residence time on normal sites, i.e., when the rate of living the defect (state 4) obeys $b \ll a, c$. It is also easily seen that for
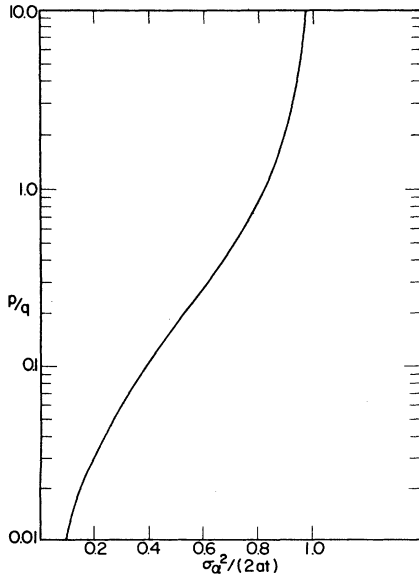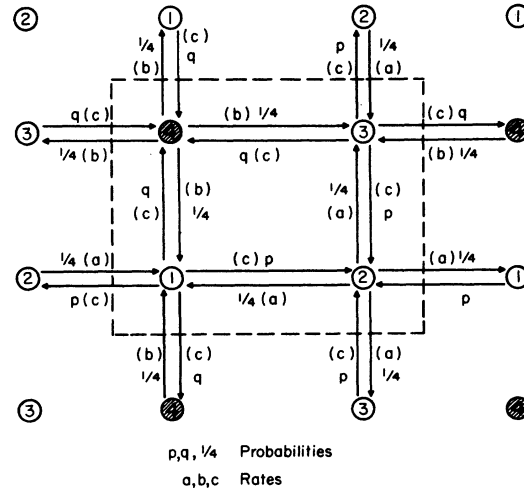
FIG. 6. Random-walk lattice where 25% of the sites have been replaced by defect sites (cross-hatched circles). The defect site is characterized by the rate of leaving it (b) and by the probability T of leaving it, such that for $T = 1$ the defect is totally reflective and for $T = 0$ totally absorbing. The unit cell is denoted by dashed lines.

given T, q, p, a, and b and $c < a, b$, the value of the variance in Eq. (5.10) is smaller than in the ideal lattice case.

We can analyze the case when leaving a particular state becomes the rate-limiting step in the diffusion by using Eq. (5.10) to find

$$\lim_{a \to 0} \sigma_x^2 = \frac{4a}{p} t, \tag{5.12a}$$

$$\lim_{b \to 0} \sigma_x^2 = \frac{2b}{q} t, \tag{5.12b}$$

$$\lim_{c \to 0} \sigma_x^2 = 4ct, \tag{5.12c}$$

while the case of $b \to 0$ or $T \to 0$ is given in Eq. (5.11).

While a more complete analysis of the above and the investigation of the effects of defect concentration and lattice topology on clusters are the subjects of a separate study,[36] we have demonstrated in this section the principles of the extension of our method to treat the motion of particles on defective lattices, and the new trends characteristic of particle migration on these lattices.

VI. CONCLUSIONS

We have presented in this paper a formalism, based on stochastic techniques, for the description of the propagation of a system with internal states on a lattice. The model we have used is a continuous-time random walk with internal states. In this study the internal states are the allowed spatial configurations of a cluster of atoms migrating on a crystalline surface. The random-walk lattice is constructed via a mapping of the locations of the cluster centroid onto a periodic lattice.

The random-walk lattice sites need not represent spatial displacements of the system variables. In general, sites of the random-walk lattice may correspond to a set of states which characterize the evolution of the system, i.e., intermediate states on a reaction coordinate.

In Sec. II B we have provided a concise procedure for the application of our formalism to systems of arbitrary complexity. We have applied our formalism to the diffusional motion of 2- and 3-state dimers in one dimension and a 3-state dimer in two dimensions. The effect of a bias field on the motion has been included. We have derived expressions for the mean and variance of cluster displacement and equilibrium probabilities of occupation of states. Using these results, we have expressed the transition rates between the allowed configurations (states) in terms of *observable* quantities, thus enabling a *complete determina-*

tion of the *individual* activation energies and frequency factors of transitions between states from experimental data. We have demonstrated that in certain cases (e.g., 3-state dimer in one dimension) such a complete determination necessitates migration experiments with a bias field. In certain other cases (e.g., 3-state dimer in two dimensions) we provide more relations than there are transition rates. Consequently, several alternative methods of analysis of experimental data are given, allowing consistency checks and the investigation of the effect of a bias field on activation energies and frequency factors.

The analysis of the motion of higher-order clusters becomes more involved owing to the occurrence of a large number of allowed states; for example, in one dimension the motion of a trimer with transitions to nearest-neighbor sites is characterized by six distinct states connected by nine independent transition rates. (This calculation will be reported elsewhere.) In addition, our formalism can be reduced to a computational algorithm which allows the analysis of the dynamics of complex clusters. We are currently investigating, using our formalism, models of the kinetics of thin-film growth, annealing, and diffusion-controlled surface reactions.

In Sec. V we have presented an extension of our method to treat the influence of defects on the motion. We have illustrated the effect of periodically placed defects (totally or partially reflecting) on the motion of a single particle on a four-fold-coordinated lattice. Clearly, the topology of the underlying lattice influences the motion of single particles and clusters. The effect of defects is also a function of the topology (connectivity) of the lattice. In attempting to optimize the diffusion rate (minimize the *poisoning*, i.e., inhibiting effect, caused by the defects) we are employing our methods for a systematic study of the diffusion on lattices of various topologies and defect concentrations.

The treatment of systems which exhibit a low concentration of periodically spaced defects by our present methods entails the inversion of a large matrix, since the unit cell will contain many sites. While in principle this can be accomplished, we have developed new methods, based upon a renormalization of the propagator due to the effect of the defects, for treating such cases.

In the description of surface reactions, certain defects may be identified as *active sites*. These active sites may be *desorption sites* to which reactive intermediate migrate,[37] or *reaction sites* on which (or in the vicinity of which) reactants interact. Our renormalized propagator technique

has been employed by us to derive kinetic expressions for such reactions. Reports on these methods and the results we obtained by their application have appeared elsewhere,[36] and will be discussed in detail in forthcoming publications.

*Work partially supported by the U. S. ERDA contract No. EG-77-S-05-5489.

†Present address: School of Physics, Georgia Institute of Technology, Atlanta, Ga. 30332.

[1]For recent reviews see the following (and references cited therein): H. D. Hagstrum and E. G. McRae, in *Treatise on Solid State Chemistry*, edited by N. B. Hannay (Plenum, New York, 1976), Vol. 5; T. N. Rhodin and D. L. Adams, *ibid.*; U. Landman and G. G. Kleiman, in *Surface and Defect Properties of Solids*, edited by M. W. Roberts and J. M. Thomas (Chemical Society, London, 1977), Vol. 6; articles in *The Structure and Chemistry of Solid Surfaces*, edited by G. A. Somorjai (Wiley, New York, 1969); articles in *Methods of Surface Analysis*, edited by A. W. Czanderna (Elsevier, Amsterdam, 1975).

[2]A collection of papers representative (though not exhaustive) of various approaches to surface phenomena can be found in *The Physical Basis For Heterogeneous Catalysis*, edited by E. Dragulis and R. I. Jaffee (Plenum, New York, 1975); see also Ref. 1.

[3]For a review of past and current trends in catalysis research, emphasizing the "interfacing" of practical and basic considerations and the importance of the development of correlation schemes, see J. B. Butt, AICE J. $\underline{22}$, 1 (1976), and references cited therein.

[4]J. M. Thomas and W. J. Thomas, *Introduction to the Principles of Heterogeneous Catalysis* (Academic, New York, 1967).

[5]J. M. Blakely, Prog. Mater. Sci. $\underline{10}$, 395 (1963); G. E. Rhead, Scr. Metall. $\underline{6}$, 47 (1972).

[6](a) P. Bennema and G. H. Gilmer, in *Crystal Growth: An Introduction*, edited by P. Hartman (North-Holland, Amsterdam, 1973), p. 263; (b) D. Elwell and H. J. Scheel, *Crystal Growth from High Temperature Solutions* (Academic, New York, 1975).

[7]The first applications of stochastic ideas to chemical kinetics is due to H. A. Kramers, Physica $\underline{7}$, 284 (1940); M. Delbrück, J. Chem. Phys. $\underline{8}$, 120 (1940). For further developments and reviews see (a) E. W. Montroll and K. E. Shuler, Adv. Chem. Phys. $\underline{1}$, 361 (1958); (b) E. W. Montroll, Energ. Metall. Phenom. $\underline{3}$, 123 (1967); (c) D. A. McQuarrie, in *Methuen's Monographs on Applied Probability and Statistics*, edited by J. Gani (Methuen, London, 1967), Vol. 8.

[8]For recent applications to surface phenomena see (a) D'Agliano, E. G. Schaich, W. L. Kumar, and H. Suhl, in *Proceedings of the 24th Nobel Symposium on Collective Properties of Physical Systems* (Academic, New York, 1973); (b) G. Iche and Ph. Nozières, J. Phys. (Paris) $\underline{37}$, 1313 (1976); (c) K. Kitahara, H. Metin, J. Ross, and R. Silbey, J. Chem. Phys. $\underline{65}$, 2871 (1976); U. Landman, E. W. Montroll, and M. F. Shlesinger, Phys. Rev. Lett. $\underline{38}$, 285 (1977).

[9]For recent reviews see (a) G. Ehrlich, Crit. Rev.

Solid State Sci. $\underline{4}$, 205 (1974); (b) D. W. Bassett, in *Surface and Defect Properties Solids*, edited by M. W. Roberts and J. M. Thomas (Chemical Society, London), Vol. 2, p. 34. (c) W. R. Graham and G. Ehrlich, Thin Solid Films $\underline{25}$, 85 (1975); (d) G. E. Rhead, Surf. Sci. $\underline{47}$, 207 (1975).

[10]E. W. Müller and T. T. Tsong, *Field Ion Microscopy* (Elsevier, New York, 1969); see also Ref. 9(a) and 9(b).

[11]U. Landman, E. W. Montroll, and M. F. Shlesinger, in Ref. 9(d).

[12]E. W. Müller, Z. Naturforsch. $\underline{11a}$, 87 (1956); J. Appl. Phys. $\underline{27}$, 474 (1956).

[13]For a most recent review see J. M. Cowley and S. Iijma, Phys. Today $\underline{30}$, 32 (1977).

[14]T. B. Grimley, Proc. Phys. Soc. London $\underline{90}$, 751 (1967); T. B. Grimley and S. M. Walker, Surf. Sci. $\underline{14}$, 395 (1969).

[15]T. L. Einstein and J. R. Schrieffer, Phys. Rev. B $\underline{7}$, 3629 (1973).

[16]See the review by T. Takaishi in *Progress in Surface Science*, edited by S. G. Davidson (Pergamon, London, 1975), Vol. 6, p. 43.

[17]T. T. Tsong and R. J. Walko, presented at the Nineteenth Field Emission Symposium, Urbana, Ill., 1972 (unpublished).

[18](a) W. R. Graham and G. Ehrlich, Phys. Rev. Lett. $\underline{31}$, 1407 (1973); (b) J. Phys. F $\underline{4}$, L212 (1974).

[19]W. R. Graham and G. Ehrlich, Phys. Rev. Lett. $\underline{32}$, 1309 (1974).

[20]D. A. Reed and G. Ehrlich, Philos. Mag. $\underline{32}$, 1095 (1975).

[21]T. Sakata and S. Nakamura, Surf. Sci. $\underline{51}$, 313 (1975).

[22]K. Stolt, W. R. Graham, and G. Ehrlich, J. Chem. Phys. $\underline{65}$, 3206 (1976).

[23]T. T. Tsong, P. Cowan, and G. Kellogg, Thin Solid Films $\underline{25}$, 97 (1975).

[24]D. W. Bassett, J. Phys. C $\underline{9}$, 2491 (1976).

[25]D. W. Bassett, Surf. Sci. $\underline{21}$, 181 (1970); D. W. Bassett and M. J. Parsley, Nature $\underline{221}$, 1046 (1969).

[26]D. A. Reed and G. Ehrlich, J. Chem. Phys. $\underline{64}$, 4616 (1976).

[27]U. Landman, E. W. Montroll, and M. F. Shlesinger, Proc. Natl. Acad. Sci. USA $\underline{74}$, 430 (1977).

[28]E. W. Montroll and G. H. Weiss, J. Math. Phys. (N.Y.) $\underline{6}$, 167 (1965).

[29]H. Scher and M. Lax, Phys. Rev. B $\underline{7}$, 4491 (1973); $\underline{7}$, 4502 (1973).

[30]E. W. Montroll and H. Scher, J. Stat. Phys. $\underline{9}$, 101 (1973).

[31]M. F. Shlesinger, J. Stat. Phys. $\underline{10}$, 421 (1974).

[32]G. E. Roberts and H. Kaufman, *Tables of Laplace Transforms* (Saunders, Philadelphia, 1966), Sec. 3.

[33]In our analysis we have not included effects due to the finite size of the crystal plane on which migration is

taken place [in their study of Re motion on W(211), Stolt *et al.* (Ref. 22) estimate the size of a plane to be of the order of ≈ 25 binding sites per diffusion channel]. The interaction of the migrating particle with the boundary can be of a reflective type [as was observed for tungsten atom diffusion on W by G. Ehrlich and F. G. Hudda, J. Chem. Phys. **49**, 1039 (1966), and by D. W. Bassett and M. J. Parsley, J. Phys. D **3**, 707 (1970)] or of an absortive type (see Ref. 22). In any case one can correct the experimental measurement for such events (see, for example, the discussion in Sec. I D 2 of Ref. 22) or carefully omit such events from the data [for example, in the experimental coi. figuration of Stolt *et al.* (Ref. 22) only jumps starting from the central one-half of the channel were counted, in order to eliminate edge effects].

[34]C. P. Flynn, *Points Defects and Diffusion* (Clarendon, Oxford, 1972).

[35]S. Nisigaki and S. Nakamura, Jpn. J. Appl. Phys. **15**, 1647 (1976).

[36]U. Landman and M. F. Shlesinger, in *Proceedings of the Thirteenth IUPAP Conference on Statistical Physics, 1977* Annals of the Israel Phys. Soc., Vol. 2, edited by C. Kuper and I. Reiss; in Abstracts of the 37th Annual Conference on Physical Electronics, Stanford, 1977 (unpublished); and unpublished. In the above reports we describe a method based upon a renormalization of the propagator due to the defects. The method allows us to derive expressions for the spatial moments and occupation probabilities for arbitrary defect concentration and surface structure. The method is well suited for the treatment of systems with low defect concentration, for which case other methods are computationally prohibitive. One of the important findings of the above studies is the surface structure dependence of diffusion rates when the defect influences transition rates from its neighbors. It should be noted that the formalisms described in the present paper and the renormalized propagator method for treating systems which contain defects can be applied with an appropriate identification of terms to other transport problems (for example, exciton migration and spin diffusion in perfect and defective crystals).

[37]R. J. Madix, J. Vac. Sci. Technol. **13**, 253 (1976).